J Low Temp Phys (2008) 151: 690–696
DOI 10.1007/s10909-008-9729-2

A Kilopixel Array of TES Bolometers for ACT: Development, Testing, and First Light

M.D. Niemack · Y. Zhao · E. Wollack · R. Thornton · E.R. Switzer · D.S. Swetz · S.T. Staggs · L. Page · O. Stryzak · H. Moseley · T.A. Marriage · M. Limon · J.M. Lau · J. Klein · M. Kaul · N. Jarosik · K.D. Irwin · A.D. Hincks · G.C. Hilton · M. Halpern · J.W. Fowler · R.P. Fisher · R. Dünner · W.B. Doriese · S.R. Dicker · M.J. Devlin · J. Chervenak · B. Burger · E.S. Battistelli · J. Appel · M. Amiri · C. Allen · A.M. Aboobaker

Received: 23 July 2007 / Accepted: 15 September 2007 / Published online: 24 January 2008

Abstract The Millimeter Bolometer Array Camera (MBAC) will be installed on the 6-meter Atacama Cosmology Telescope (ACT) in late 2007. For the first season of observations, MBAC will comprise a 145 GHz diffraction-limited, 1024-pixel, focal plane array of Transition Edge Sensor (TES) Bolometers. This will be the largest array of pop-up-detector bolometers ever fielded as well as one of the largest arrays of TES bolometers. We discuss the design specifications for the array and pre-assembly testing procedures for the cryogenic components. We present dark measurements of the TES bolometer properties of numerous 32-pixel columns that have been assembled into the first kilopixel array for ACT, as well as optical measurements made with our 256-pixel prototype array, including first light measurements on ACT.

M.D. Niemack (✉) · Y. Zhao · E.R. Switzer · S.T. Staggs · L. Page · O. Stryzak · T.A. Marriage · J.M. Lau · N. Jarosik · A.D. Hincks · J.W. Fowler · R.P. Fisher · J. Appel
Princeton University Physics Department, Princeton, NJ 08544, USA
e-mail: mniemack@princeton.edu

E. Wollack · H. Moseley · J. Chervenak · C. Allen
NASA Goddard Space Flight Center, Greenbelt, MD 20771, USA

R. Thornton · D.S. Swetz · M. Limon · J. Klein · M. Kaul · S.R. Dicker · M.J. Devlin
University of Pennsylvania Physics Department, Philadelphia, PA 19104, USA

M. Halpern · B. Burger · E.S. Battistelli · M. Amiri
Univ. of British Columbia Dept. of Physics and Astro., Vancouver, BC V6T 1Z1, Canada

K.D. Irwin · G.C. Hilton · W.B. Doriese
National Institute of Standards and Technology, Boulder, CO 80305, USA

R. Dünner
Universidad Católica, Santiago, Chile

A.M. Aboobaker
Univ. of Minnesota School of Physics and Astro., Minneapolis, MN 55455, USA

Keywords TES · Bolometer · Detector array · Astrophysics · Cosmology

PACS 07.57.Kp · 95.55.Rg · 95.85.Bh · 95.55.Jz · 95.85.Fm · 98.80.Es

1 Introduction

The Millimeter Bolometer Array Camera will measure the Cosmic Microwave Background radiation (CMB) temperature anisotropies at small angular scales [1] on the 6-meter ACT [2]. The construction of ACT was recently completed in Chile, and engineering observations have begun with our prototype instrument, the Column Camera (CCam) [3]. We are building three 1024-pixel arrays of Transition Edge Sensor (TES) bolometers for MBAC, which are optimized for use at 145, 217, and 265 GHz. These three frequencies will allow background and point source subtraction for CMB analysis at high multipoles. In addition, they span the null of the Sunyaev-Zel'dovich (SZ) Effect—the Compton scattering of CMB photons off hot electrons in galaxy clusters. By measuring the SZ effect with these bands, we will generate an unbiased galaxy cluster catalog [1]. Combining this catalog with optical and X-ray measurements will allow us to measure cluster density as a function of redshift, which can be used to constrain cosmological parameters, including the equation of state of the dark energy that dominates our universe.

Our bolometer arrays are highly modular [4, 5], which enables us to pre-screen and choose the best components for each 32 pixel column module. Each module is comprised of 5 primary components: a TES bolometer chip, a chip of shunt resistors to voltage bias the TESs, a Nyquist inductor chip to band-limit the TES response, a superconducting quantum interference device (SQUID) multiplexing chip, and a Si circuit board with Al wiring to which all the other components are mounted [6]. Prior to assembly with detectors, the series resistance of the 32 resistors on each shunt chip and the SQUID critical currents of the multiplexing (mux) chips are characterized in a ^{4}He dip probe. The pop-up detector [7] bolometers as well as the shunt resistor chips are fabricated at NASA Goddard's Detector Development Laboratory. The bolometer response is measured using a three-stage SQUID time-domain multiplexing (TDM) system [8, 9] developed at NIST, Boulder, where the Nyquist inductor chips are also fabricated. The Si circuit boards are fabricated at Princeton, where components are tested and built into arrays (Fig. 3b).

In this paper we give a general description of the detector and parameter selection for these arrays. Then, we present dark measurements of bolometer properties for MBAC made in two rapid dip probe refrigerators [4]. We also present optical measurements of detectors in our prototype array made in CCam using the Multi-Channel Electronics (MCE) [11] and conclude with our recent first light measurements with CCam on ACT.

2 Array Design: Detector Parameter Selection

Among the variety of different measurements described here, three critical bolometer properties determine the functionality and sensitivity of the detector array during observations: the saturation power, the noise level, and the time constant, or frequency

Table 1 Dark measurement results from eight of the detector columns with 32 pixels each that will go into 145 GHz array. These measurements were acquired at $T_b \approx 0.38$ K, which is why the bias power, P_{J_o} is somewhat lower than discussed in Sect. 2

	T_c	R_n	R_{sh}	P_{J_o}	I_b at 0.5 R_n	*Noise* at 10 Hz
Average	0.512 K	32 mΩ	0.74 mΩ	6.5 pW	0.46 mA	4.1×10^{-17} W s$^{1/2}$
Std. Dev.	0.026 K	5 mΩ	0.10 mΩ	1.1 pW	0.04 mA	1.3×10^{-17} W s$^{1/2}$

response. The saturation power, P_{sat}, will determine whether the detectors can function without saturating during observations. The noise level impacts the ratio of photon noise to detector noise and affects the final sensitivity of the sky maps. The time constant, f_{3dB}, determines how quickly the telescope can be scanned across the sky without low-pass filtering small angular scale signals.

The selection of detector parameters for the array has been a gradual process motivated by a combination of theoretical calculations, measurements, and fabrication recipe success. The non-multiplexed SQUID noise was measured to be $\sim 0.5\ \mu\phi_o/\sqrt{\text{Hz}}$ [8], and we found that aliasing caused by multiplexing at our planned rate, $f_{samp} = 15.2$ kHz, increased the SQUID noise level by a factor of ∼8. This drove us to select a low TES normal resistance, R_n, of ∼30 mΩ to ensure that the detector current noise would dominate the TDM SQUID noise. The shunt resistance value, $\sim 0.7\ \text{m}\Omega \ll R_n$, was selected to keep the TESs roughly voltage-biased without being so small as to generate excess Joule heating in the shunt resistors that would warm up the bath temperature.

The predicted loading in the 145 GHz band on the Atacama Plateau is <2 pW during the observation season [6], which puts a lower limit on the acceptable P_{sat}. (Load curve measurements in Chile have recently confirmed this estimate.) Consideration of the measured scatter in detector parameters (Table 1), our desire to bias the entire kilopixel detector array with only a few bias lines, and the results of time constant measurements (Sect. 4) drove us to choose a substantially higher P_{sat}. Aside from its dependence on the bath temperature, P_{sat} depends on the TES transition temperature, T_c and the thermal conductivity, G, of the weak link to the bath. The dependence of the latter two on fabrication recipes are determined by laboratory measurements [4]. For the 145 GHz array, the bolometers have four 5 μm wide × 1.1 μm thick × 0.5 mm long Si legs connecting them to the ∼0.3 K bath and $T_c \approx 0.51$ K, resulting in $P_{sat}(0.3\ \text{K}) \approx 8$ pW.

3 Dark Detector Measurements

Each column of 32 bolometers is subjected to a series of tests prior to insertion into the array. These tests are performed on every detector and include: measurements of the SQUID V-ϕ curve through the SQUID feedback and detector bias lines; TES T_c; Johnson noise spectra to extract the shunt resistance, R_{sh}, and Nyquist inductance; load curves for TES normal resistance, R_n, saturation power, P_{sat} and bias current, I_b; multiple noise measurements on the transition to measure non-multiplexed noise spectra and check for anomalies (Table 1). Based on these measurements, columns

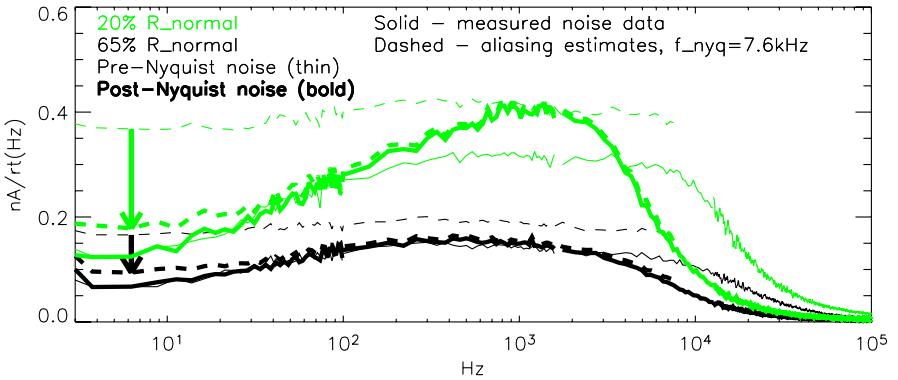

Fig. 1 (Color online) Comparison of noise measurements (*solid*) and aliasing estimates (*dashed*) pre-Nyquist inductors (*thin lines*) vs. post-Nyquist inductors (*bold lines*) at 0.2 R_n (*green*—the top three curves) and 0.65 R_n (*black*). Thick *vertical arrows* near 6 Hz indicate the estimated reduction of in band aliasing by adding the Nyquist inductor into the TES loop

for the final array have typically had a 90% pixel yield. The few bad pixels on each column are caused by a variety of different failure modes, including: mechanically broken pixels, unresponsive or open stage 1 SQUIDs, electrical shorts on the TES or the mux chip, and oscillating detectors at certain biases.

Noise and complex impedance measurements of the bolometers indicate that thermally they comprise at least three elements with isolated heat capacities. Dünner has led an effort to model this system. He found that the noise and impedance data can be explained well by a model in which the TES and ion-implanted absorber heat capacities are thermally isolated and connected to the bath through the bolometer Si. This seems appropriate since these bolometers have a small TES (50 μm × 50 μm) separated from a thin absorber layer by the relatively large (1.05 mm × 1.05 mm × 1.1 μm) bulk Si.

The isolated heat capacities and the resulting increase in noise in the mid-frequency range (Fig. 1) should not pose a problem so long as the noise is prevented from aliasing into our low-frequency sky sampling band. Adding inductance into the TES loop reduces aliasing by decreasing the frequency of the L/R electrical pole below the Nyquist sampling frequency, $f_{Nyq} = f_{samp}/2 = 7.6$ kHz. Due to the complexity of the bolometer model, we determined the inductance experimentally using a NIST multi-L chip with values between $L = 0.1$–1.4 μH. The noise on each bolometer was measured at multiple bias points before and after adding the inductor (Fig. 1). The noise level after aliasing, $N_a(f)$ where f is a frequency between 0 Hz-f_{Nyq}, was estimated before and after adding the inductor by folding the measured power spectral density (PSD), $N_m(f)$, about f_{Nyq}: $N_a(f) = \sum_{i=0}^{k} N_m(2if_{Nyq} + f(-1)^i)$. We sum over $i = 0 \rightarrow k$ folds, where k is an integer that meets the condition: $N_m(2kf_{Nyq} + f(-1)^k) \ll N_a(f)$ for k and integers greater than k. Aliasing estimates in Fig. 1 were summed to $k = 4$, or 38 kHz.

To select the optimal inductance, we found the maximum decrease of in-band aliased noise that occurred after introducing the inductor. Above the optimal inductance, detectors tend to either have an increase in low-frequency noise or be driven

into oscillations. Due to the scatter in our detector properties, we chose an inductance 15% below the optimal value, resulting in a total circuit inductance of ∼0.75 μH. This has been a successful approach in that we often find a single detector in each 32-pixel column that is driven into an unstable resonant state at some biases, but there is rarely more than one per column. Wirebonds are disconnected from detectors that exhibit resonant behavior to prevent oscillations from contaminating the signals on neighboring detectors.

We are in the process of testing a Si coupling layer design that optimizes the optical impedance of the bolometers to match free space. The layer resembles an evanescently coupled anti-reflection coating. Calculations indicate that such a layer can yield close to 80% radiation efficiency.

4 Optical Time Constant Measurements

Our observation strategy is to scan the entire telescope in azimuth 5° peak-to-peak [2]. The angular velocity of this scan imposes a lower limit on the detector f_{3dB} to prevent filtering of the beams at high frequencies [3]. Measurements of the detector time constants of the bolometers in the prototype 8 × 32 array were made by chopping a 300 K Ecosorb source in front of a small aperture near a focus of the CCam dewar at numerous frequencies. A 9% transmissive neutral density filter was in the dewar optical path to prevent saturation of the bolometers. All measurements were made in a multiplexed mode using the MCE [11] for data acquisition.

The data were analyzed by Fourier transforming the time streams, integrating over the peak response to the chopper and subtracting the background PSD. Bolometer f_{3dB} was calculated from a single-pole fit to the frequency response. Load curves acquired before and after each series of measurements confirmed system stability and provided detector parameters at the 10-20 biases studied.

Based on an isothermal TES bolometer model in the low inductance limit, we would expect [10]

$$f_{3dB} = \frac{G}{2\pi C}\left(1 + \frac{(1 - R_{sh}/R_o)\alpha_I}{(1 + \beta_I + R_{sh}/R_o)GT_o}P_{J_o}\right),$$

where P_{J_o} is the Joule power applied to the TES and R_o is the TES resistance (parameter definitions follow the conventions of Irwin and Hilton [10].) The low-inductance limit is an acceptable approximation, despite our use of Nyquist inductors, because the L/R electrical time constant is roughly an order of magnitude smaller than the optical time constants. With other parameters held constant, f_{3dB} is proportional to P_{J_o}. Measurements of two columns of prototype detectors and one column of detectors for the first array follow this trend (Fig. 2). The bolometers also have roughly constant f_{3dB} between 25%–75% of R_n, indicating changes in the parameters C, α_I, and β_I do not have a strong impact on f_{3dB} in this regime. These measurements were made in the laboratory at elevated bath temperatures and loading; however, by combining this function with G measurements, we can estimate f_{3dB} under observing conditions. We will study time constant stability during observations by both scanning quickly across point sources and measuring bolometer responses to square wave steps on the detector bias line using the MCE [11].

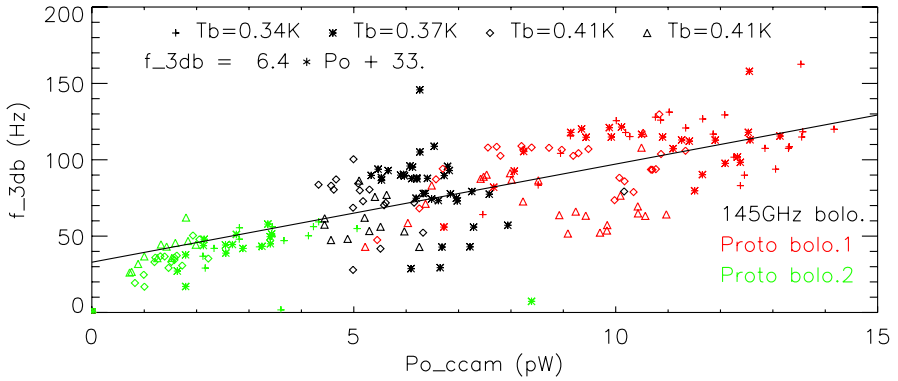

Fig. 2 (Color online) Time constants of 3 different types of bolometers measured at 3 bath temperatures at $R_o \approx 0.5R_n$ follow the trend $f_{3dB} \approx (6.4\ \text{Hz/pW})P_{J_o} + 33\ \text{Hz}$

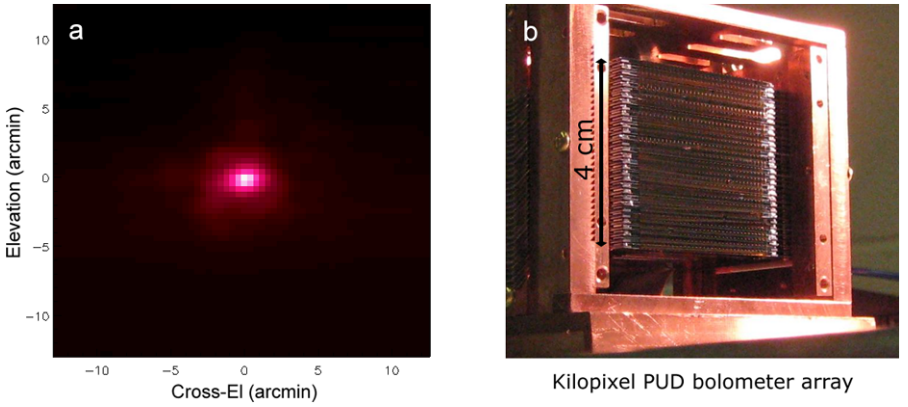

Fig. 3 (Color online) **a** CCam first light map of Jupiter (Sect. 5). **b** The first kilopixel array for MBAC

5 First Light

We have recently made a first light measurement with CCam on ACT. Jupiter was measured with our prototype array during an azimuthal scanning observation. These observations indicate that our focal plane plate scale is $\sim 38'/\text{mm}$, which was expected for CCam on ACT. However, when these data were acquired CCam had not been focused, the alignment of the primary mirror was not completed, and the optics in CCam were optimized for use with another telescope design. Thus, the image in Fig. 3a should not be taken as representative of the image quality we expect to achieve with our first array (Fig. 3b) in MBAC in the near future. Telescope alignment and observations continue with CCam, while the testing of the kilopixel 145 GHz array is completed for the upcoming MBAC deployment.

Acknowledgements We would like to thank all members of the ACT collaboration, especially A. Dahlen, B. Harrop, T. Essinger-Hileman, K. Martocci, L. Parker, and A. Sederberg for assistance with chip screening, testing, fabrication, and array assembly, and C. Tucker and P. Ade at Cardiff University for providing filters for CCam. This work was supported by the U.S. National Science Foundation through awards AST-0408698 for the ACT project and PHY-0355328. Princeton University and the University of Pennsylvania also provided financial support.

References

1. A. Kosowsky, New Astron. Rev. **47**, 939–943 (2003)
2. J. Fowler, M. Niemack, S. Dicker et al., Appl. Opt. **45**, 3746 (2006)
3. M. Niemack, Proc. SPIE **6275**, 62750 (2006)
4. T. Marriage et al., Nuclear Instrum. Methods Phys. Res. A **559**, 551–553 (2006)
5. J. Lau, Princeton Univ. doctoral thesis, 2007
6. T. Marriage, Princeton Univ. doctoral thesis, 2006
7. D. Benford et al., Proc. SPIE **5498**, 647 (2004)
8. P.A. de Korte et al., Rev. Sci. Instrum. **74**(8), 3807–3815 (2003)
9. C. Reintsema et al., Rev. Sci. Instrum. **74**, 4500 (2003)
10. K. Irwin, G. Hilton, *Cryogenic Particle Detection* (Springer, Berlin, 2005)
11. M. Halpern et al., Proc. LTD **12**, T03 (2007)